Lasers in Manufacturing Conference 2017

Transformation of Weld Seam Geometry in Laser Transmission Welding by Using an Additional Integrated Thulium Fiber Laser

Anton Schmailzl[a,*], Bastian Geißler[b], Frederik Maiwald[a], Tobias Laumer[b], Michael Schmidt[b,c,d], Stefan Hierl[a]

[a]*Ostbayerische Technische Hochschule Regensburg, Galgenbergstraße 30, 93053 Regensburg, Germany*
[b]*Bayerisches Laserzentrum GmbH (blz), Konrad-Zuse-Straße 2-6, 91052 Erlangen, Germany*
[c] *Erlangen Graduate School in Advanced Optical Technologies (SAOT), Paul Gordan Straße 6, 91052 Erlangen, Germany*
[d]*Chair of Photonic Technologies, Friedrich-Alexander-Universität Erlangen-Nürnberg, Paul-Gordan-Straße 3, 91052 Erlangen, Germany*

Abstract

Laser transmission welding is a well-known joining technique for thermoplastics. By using a single laser source with a wavelength close to one micron, the laser radiation is transmitted through the upper joining partner almost loss-free and afterwards absorbed in the below placed absorbent polymer. By this, the majority of the molten volume of the weld seam is located in the below placed joining partner. Furthermore, the melt layer thickness in the upper joining partner is reduced in regions with an initial gap, because heat conduction is precluded in the beginning of the welding procedure. As a result, the weld seam quality varies along the weld contour. In the worst case a gap is remaining, which causes a leakage. In order to enhance the weld seam quality, a laser with a wavelength close to two micron can be used additionally. By this, a significant absorption is given in the upper joining partner, whereby gap bridging is accelerated due to thermal expansion of the upper joining partner. In this approach, a thulium fiber laser with a wavelength of 1.94 micron is used in a coaxial arrangement to a conventionally used diode laser. Welding experiments on extruded polyamide plates are performed using several different process parameter settings, whereby typical feed rates for the process variants contour and quasi-simultaneous welding are used. It is shown, that the geometry of the weld seam can be easily manipulated, by adapting the power density distribution of the thulium fiber laser. Verification studies for both process variants have shown that computational and experimental results are matching with adequate accuracy, especially for several different process parameter settings. In order to investigate the correlation between weld seam geometry and strength in further studies, the simulation can be used as a quick and reliable tool.

Keywords: laser transmission welding; gap bridging, thulium fiber laser, process simulation, hybrid welding

* *E-mail address:* anton2.schmailzl@oth-regensburg.de .

1. Introduction

Laser transmission welding is a common joining technique for thermoplastics and used for many years in the automotive and medical industry as well as for consumer products. In order to enhance the weld seam quality in case of tightness, joint strength and residual stresses, the gap-bridging capability has to be improved, since an insufficient gap-bridging capability leads to thermal degradation (Bates et al., 2015), interruptions in the weld seam or to a reduced joint strength (Aden et al., 2013 and Devrient et al., 2013).

In order to improve gap-bridging, it is suggested in Chen et al., 2011 to use in general a high laser power and a comparatively low carbon black content in the below placed joining partner, because this leads to a high thermal expansion. Another possibility for improving the gap-bridging capability is to oscillate the laser beam, in order to enlarge the heat affected zone in the below placed joining partner (Aden et al., 2013). By this, gaps up to 75 µm can be bridged for welding PA6 in contour welding, which is an improvement by a factor of 1.97 (Devrient et al., 2013). A quite common technique is to use a secondary irradiation source with polychromatic spectrum, which is suggested in Hofmann et al., 2005 and still used for several years in industry, especially for complex formed automotive tail lights (Schmailzl et al., 2013). The highest amount of the secondary radiation is transmitted through the upper joining partner, caused by the typically used polychromatic spectrum of the emitter. By this, the below placed carbon black filled joining partner is heated in front of the laser beam as well as behind, which causes a significant reduction of the stiffness of the joining partner nearby the clamping roll. The radiation in the infrared is absorbed in the upper joining partner and leads to a warming, whereby also the stiffness is reduced. Both effects are enhancing the gap-bridging capability (Hofmann, 2006). However, the process optimization potentials are restricted so far a polychromatic emitter is used, because of the fact that a large spot of several millimeters is given, which limits precise heating in the joining zone. In order to overcome the above mentioned limitation, a laser in the spectral range of approx. 1.4 … 2.3 µm can be used as a secondary irradiation source instead of the polychromatic one. Besides the usage for contour welding, a coaxial coupled laser source can be used also in combination with scanners, which are typically used for quasi-simultaneous welding. In this approach, a thulium fiber-laser (λ = 1.94 µm) is coaxially coupled with a conventionally used diode laser (λ = 0.92 … 1.0 µm) and guided as well as focused by a 2D-scanner with f-theta lens.

However, the additional laser source makes an experimental based process analysis more difficult, because even more process parameter are given. On the other hand, a quick and reliable comparison of the effect of different parameter settings is possible by using a process simulation. So far the influence of a single parameter e.g. on the weld seam geometry is derived in a simulation and verified by experiments, the process simulation can be easily used for another welding application, even though an experimental setup does not necessarily have to exist.

The computation of the temperature field is still used for process development in contour welding (Schkutow et al., 2016 and Majumdar et al. 2015) and quasi-simultaneous welding (Wilke et al., 2008 and Piili et al., 2009). In both cases the material properties, especially the optical properties, are playing a crucial role (Geiger et al., 2009). Especially the heat conductivity and the thermal capacity have to be considered as temperature dependent, because of their influence on the weld seam geometry (Potente et al., 2008). Also the heat conductance between the joining partners has an influence on the resulting weld seam geometry, as investigated in Liu et al., 2015. Especially for the computation of residual stresses a thermo-mechanical coupled simulation is needed, which is already used in Zoubeir et al., 2010 and Sooriyapiragasam et al., 2016. However, emerging gaps between the joining partner, caused by thermal expansion, and especially their effect on the resulting weld seam geometry is not investigated.

At first, welding experiments are performed in order to analyze the effect of a secondary laser on the weld seam geometry. Secondly, a thermo-mechanical coupled simulation is built with a detailed view on the

local heat conductance in between the joining partner. Finally, the weld seam geometry is compared with simulation results in order to verify the process model.

2. Laser Welding Equipment

The experimental setup consists of a breadboard, where the collimators of the two laser sources are mounted (fig. 1). The primary laser is a diode laser (TrueDiode 301, Trumpf Laser). The laser source emits at a wavelength range of 920 … 1050 nm, its maximum output power is 300 W (cw) and the beam quality is M^2 = 22.7. The secondary laser source is a thulium fiber-laser (TLR-50, IPG) with a maximum output power of 50 W (cw), a wavelength of 1940 nm and a beam quality of M^2 = 1.1. Two mirrors are used for each laser beam in order to get a coaxial configuration at the dichroic mirror, where the laser beams are combined. For deflection and focusing of both laser beams a galvanometer scanner (PS1-10, Cambridge Technologies) and a non-color corrected f-theta lens (S4LFT3162, Sill Optics) with an effective focal length of 163 mm are used. A beam expander is integrated in the beam path of the thulium fiber-laser to enable the adjustment of the beam diameter in the joining plane relative to the beam diameter of the diode laser. The whole setup is mounted on a motorized z-axes, which allows the variation of the distance between the f-theta lens and the workpiece. The samples are positioned in an overlap and fixed by a pneumatic clamping device. The used joining pressure is 2 N/mm² for an overlap area of 20 x 30 mm. The experimental setup with the clamping technology and the sample geometry is shown schematically in fig. 1.

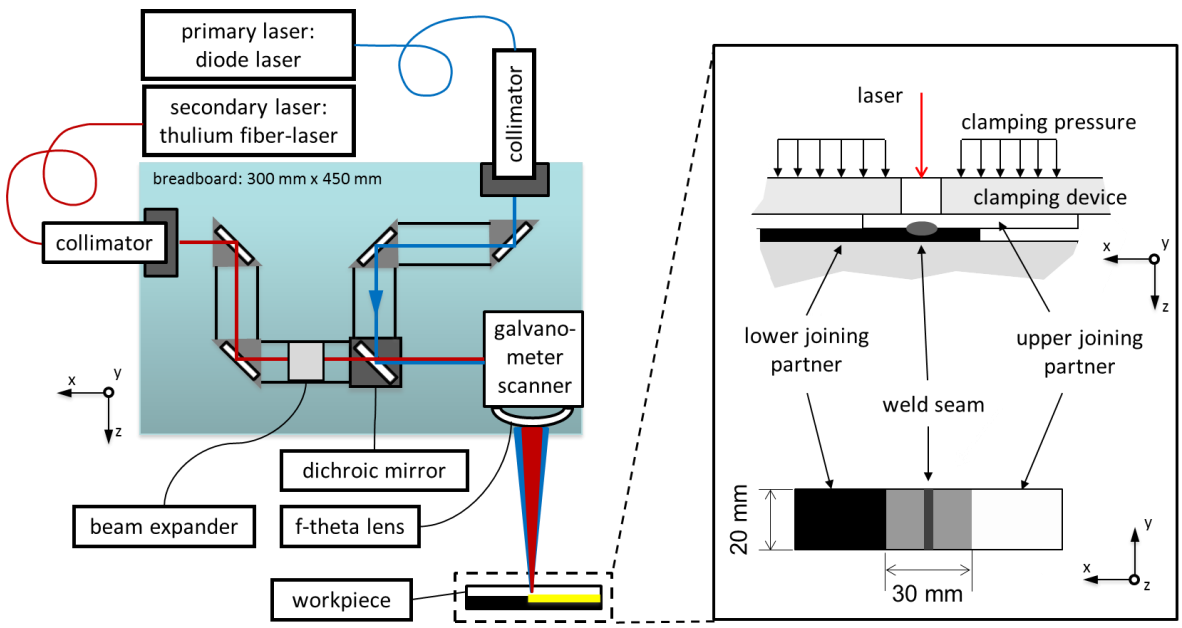

Fig. 1. Experimental setup for laser transmission welding with a conventional diode laser as well as with a thulium fiber-laser (left), clamping technology and sample geometry (right)

Preliminary investigations of the wavelength dependent absorption behavior for different unfilled thermoplastics have shown that PA6 has a high absorption coefficient (α = 0.98 1/mm) for the wavelength of the thulium fiber-laser compared to PMMA (α = 0.24 1/mm), PE (α = 0.35 1/mm), PC (α = 0.09 1/mm) or PP (α = 0.29 1/mm). Because of the high absorption and the frequent use in the automotive industry PA6 is chosen for further simulative and experimental investigations.

3. Thermo-Mechanical Process Model

3.1. Thermo-Mechanical Coupling

In a first approximation, both analyses the thermal and the mechanical can be performed one after another, whereby transient effects are considered in the thermal and neglected in the mechanical. Initially, the temperature field is computed based on the volumetric heat by solving Fourier's heat equation (fig. 2, top left). In the following, the temperature field is transferred to the mechanical analysis, where the deformation is computed on basis of the temperature dependent stiffness and the applied clamping force (fig. 2, top right). Also, the change in volume, due to the thermal expansion, has to be taken into account, which is done by using a thermal expansion coefficient. Since the volumetric heat is not homogeneous in the joining zone, especially lateral to the optical axes, the thermal expansion leads to an emerging gap (fig. 2, top right), which has to be taken into account, since it affects the heat conductance in between the joining partner. Hence, it is distinguished between contact and non-contact based on a criterion for the separation (s_c) in between the joining partner (fig. 2, bottom). In contact regions an ideal heat conductance is assumed, whereby the thermal contact conductance coefficient is set to infinity. As far as a gap greater than e.g. 10 microns occurs, the thermal contact conductance coefficient is set to 0 (fig. 2, bottom). The locally adjusted contact setting is then used to perform the thermal analysis again. This computation procedure is repeated until the end of welding is reached.

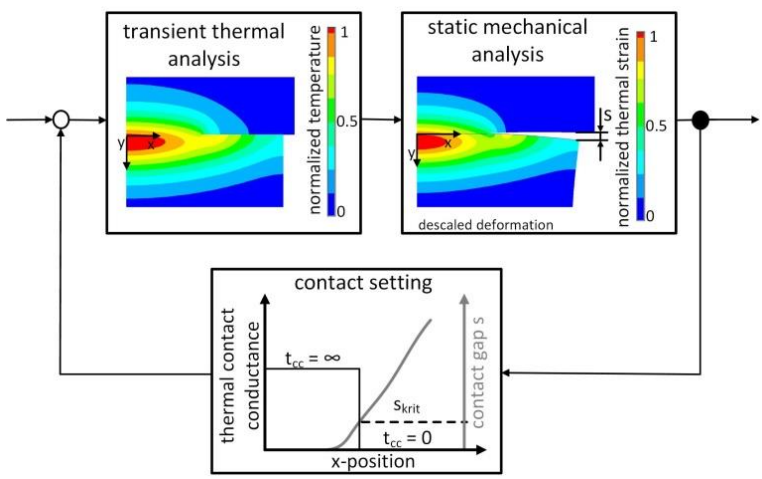

Fig. 2. Flow chart of a thermo-mechanical coupled process simulation for laser transmission welding

Besides the ideal modelling of material properties, boundary conditions and constraints, a precise consideration of the applied clamping force as well as the volumetric heat is of great importance.

3.2. Computation of Volumetric Heat

The volumetric heat is computed for a discretized volume for both joining partners and lasers on the basis of the volumetric heat equation, derived in Geiger et al., 2009. Therefore, the absorption coefficients for both joining partners have to be known. For the upper joining partner it is $\alpha_{D,u} = 0.2\ 1/mm$ for the primary laser, which is the diode laser, and $\alpha_{Th,u} = 0.98\ 1/mm$ for the secondary laser. In the below placed joining partner the absorption coefficient of $\alpha_{D,l} = 24\ 1/mm$ is derived for the primary laser and $\alpha_{Th,l} =$

15 $1/mm$ for the secondary laser. The volumetric heat in both joining partners for the primary and the secondary laser as well as for the combination of both lasers is shown exemplarily in fig. 3 (from left to right). It is assumed that the course of the power density distribution is equal for both lasers and does not change in direction of the laser beam propagation.

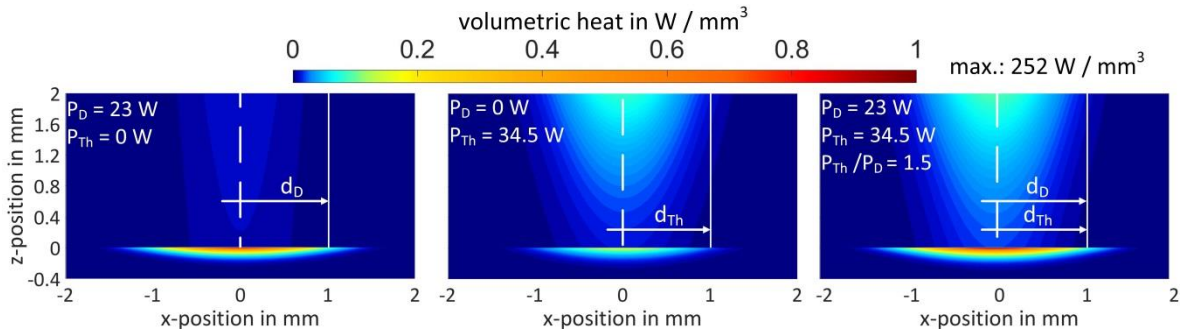

Fig. 3. Volumetric heat for a contour welding of PA6 with a conventional diode laser (left), a thulium fiber-laser (middle) as well as for the combination of both lasers at a laser power ratio P_{Th} / P_D = 1.5

The volumetric heat in the upper joining partner is insignificant for using the diode laser (fig. 3, left) and high for using the thulium fiber-laser (fig. 3, middle). In general, by using a 2 mm PA6 plate, the irradiation of the thulium fiber-laser mainly affects the upper joining partner close to the surface. It is obvious, that the computed volumetric heat in the below placed joining partner is increased by combining both lasers (see. fig. 3, right). The proportion of the intensity from the secondary laser which reaches the below placed joining partner is given by the grade of transmittance, which is $\tau_{Th} = 13.5\ \%$. However, a laser power limit is existing for the secondary laser, since melting occurs at a specific intensity at the upper surface of the upper joining partner. In consequence, the volumetric heat in the below placed joining partner is not significantly increased in a typical process parameter setting by using an additional thulium fiber-laser (fig. 3, right).

4. Transformation of Weld Seam Geometry

Welding experiments are performed for the process variants contour welding and quasi-simultaneous welding with and without a secondary irradiation, in order to investigate the effect of an additional thulium fiber-laser on the weld seam geometry. The resulting weld seam geometry is measured afterwards in thin-cuts. Based on that, the experimental datasets are used to verify the results derived by the simulations.

4.1. Contour Welding

In order to investigate the influence of the thulium fiber-laser on the weld seam geometry, the laser power of the primary diode laser (P_D) is held constant at 12.5 W and the laser power of the secondary thulium fiber-laser (P_{Th}) is increased in four steps from 0 to 25.0 W. The feed rate (v) is kept constant, as well as the laser beam diameter of the diode laser (d_D) and the beam diameter of the thulium fiber-laser (d_{Th}). The resulting weld seam geometry is exemplarily shown for three parameter sets in figure 4.

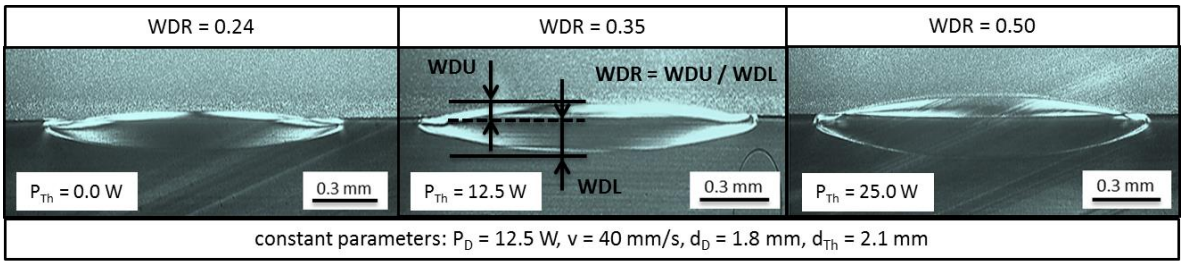

Fig. 4. Thin-cuts of contour-welded PA6 samples with derived weld depth ratio WDR (WDU = weld depth in upper part, WDL = weld depth in lower part, P_D = laser power diode laser, d_D = beam diameter diode laser, P_{Th} = laser power thulium fiber-laser, d_{Th} = beam diameter thulium fiber-laser, v = feed rate)

Due to the additional energy input of the secondary laser, the overall dimensions (width and depth) of the weld seam increases (fig. 4, from left to right). However, the depth of the weld seam in the upper joining partner (WDU) shows a stronger increase than the depth of the weld seam in the below placed joining partner (WDL), which leads to an increased weld depth ratio from 0.24 (P_{Th} = 0 W) to 0.50 (P_{Th} = 25.0 W). This indicates that the additional use of the secondary thulium fiber-laser shifts the weld seam towards the upper joining partner. In the following, the resulting weld depth ratios are compared with the results from the simulations (fig. 5).

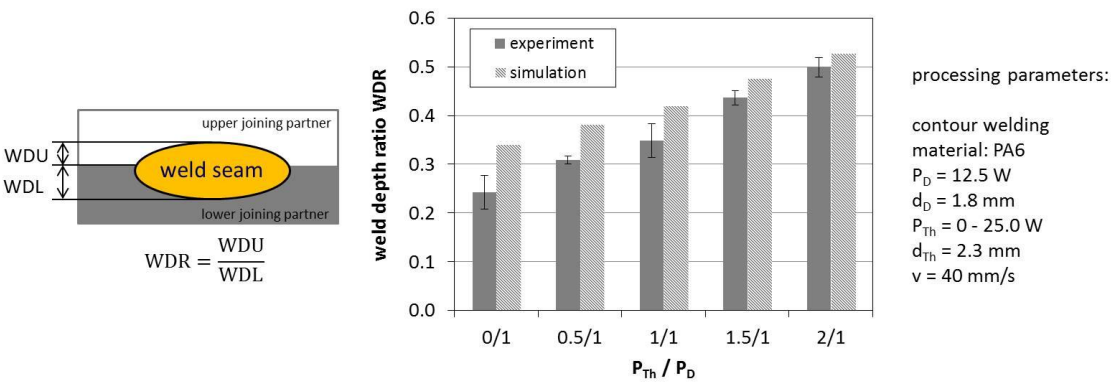

Fig. 5. Comparison of the weld depth ratios between experiment and simulation (P_D = laser power diode laser, d_D = beam diameter diode laser, P_{Th} = laser power thulium fiber-laser, d_{Th} = beam diameter thulium fiber-laser, v = feed rate, WDU = weld depth upper joining partner, WDL = weld depth lower joining partner, WDR = weld depth ratio)

The deviation between the experimental obtained weld depth ratios and the weld depth ratios from the simulation is varying between 5 % (P_{Th} / P_D = 2/1) and 36 % (P_{Th} / P_D = 0/1). For all parameter sets a higher weld depth ratio is obtained in the simulation compared to the experiment. This is probably due to the fact that an ideal thermal contact between the joining partners is assumed in the simulation as far as the joining partners are in contact, which is obviously not given in the experiment. By this, the heat flow from the below placed joining partner to the upper one is reduced in the experimental results. The above mentioned deviation increases slightly for decreasing laser power ratios (P_{Th} / P_D = 2/1 to P_{Th} / P_D = 0.5/1), because here the thermal contact zone is in general smaller compared to welds with higher laser power ratios. Obviously, the heating of the upper joining partner close to the joining zone as well as the thermal expansion of the upper joining partner caused by the secondary laser improves the thermal contact. In conclusion, it can be

stated that the model represents the increasing weld depth ratio caused by an increasing laser power ratio with adequate accuracy.

4.2. Quasi-Simultaneous Welding

Since the time dependent heating at quasi-simultaneous welding is different compared to contour welding, the welding experiments for quasi-simultaneous welding are performed with different numbers of scan repetitions. The aim is to analyze the weld seam geometry in dependence on the welding time. The welding experiments are performed without and with thulium fiber-laser at the max. laser power (P_{Th} = 50 W).

As seen, the weld depths (fig. 6, left column, top and middle) as well as the weld depth ratio (fig.6, left column, bottom) increases in dependence on the number of scan repetitions for using a conventional diode laser as well as for using a secondary laser in addition. At the highest number of scan repetition, the weld depth in both partners has nearly the same magnitude for using a secondary laser additionally, which is shown by a weld depth ratio close to 1 (WDR = 0.82). A weld depth ratio greater than approx. 0.6 can be reached only by using the thulium fiber-laser additionally, since the execution of further scan repetitions for the welding configuration without thulium fiber-laser would lead to a thermal damage of the weld seam. This indicates that the heating in the upper joining partner, caused by the secondary laser source, is enlarging the weld seam in direction of the upper joining partner.

The weld width in the upper joining partner is also still higher for the welding with thulium fiber-laser (fig. 6, right column, top). Whereas, the weld width in the below placed joining partner has nearly the same magnitude for welding with and without the thulium fiber-laser (fig. 6, right column, middle). This is expected based on the fact that the thulium fiber-laser heats the joining partner close to the optical axes, as seen by the laser beam diameter (d_{Th} = 2.1). In consequence, the weld width ratio (fig. 6, right column, bottom) is also still higher for the welding configuration with additional secondary laser. This indicates that the thermal contact in the joining zone is improved by using the thulium fiber-laser additionally, because a significant thermal expansion is given in the upper joining partner. On basis of the volumetric warming in the upper joining partner one can expect that gap-bridging is improved by an increased thermal expansion of the upper joining partner.

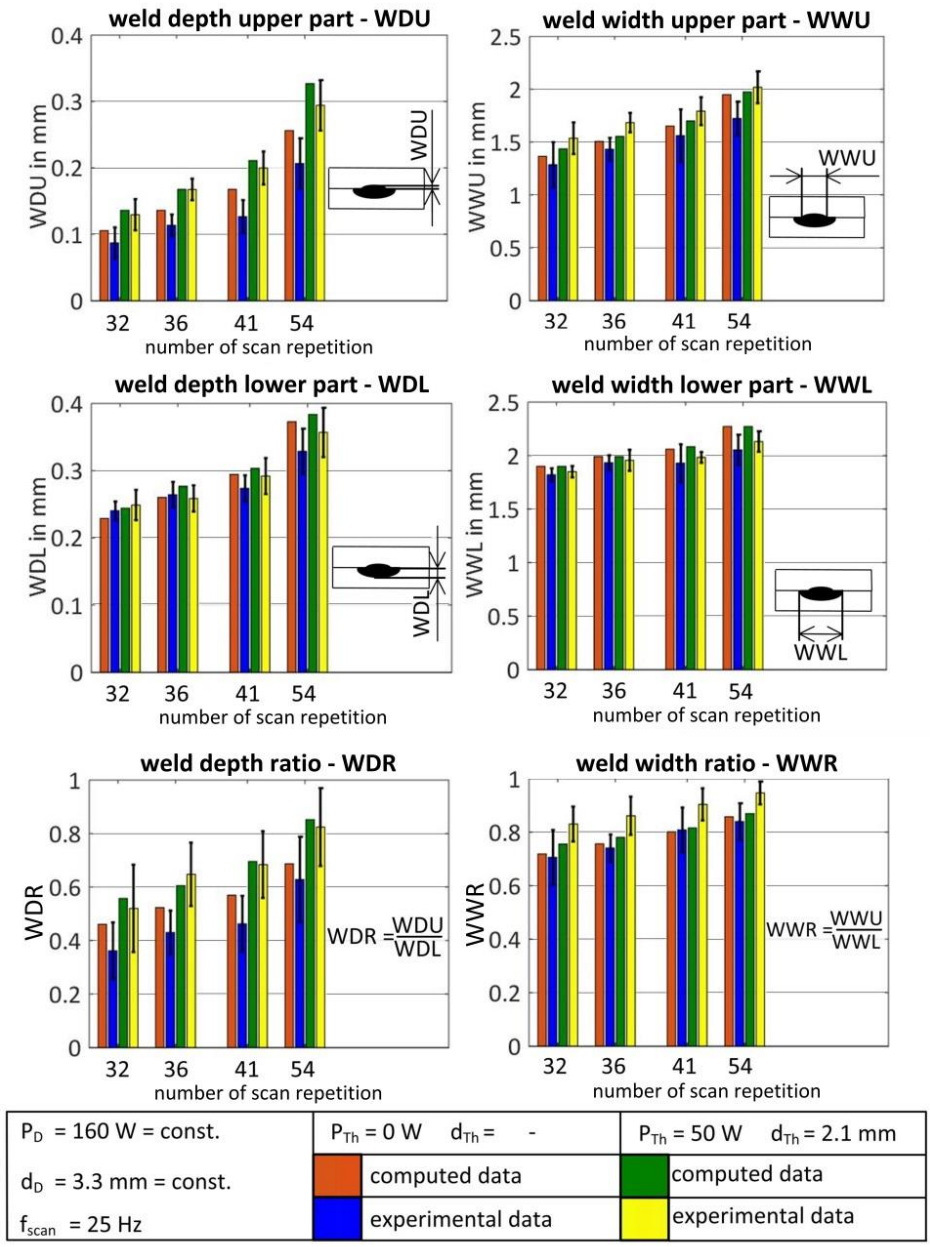

Fig. 6. Comparison between simulated and measured weld seam dimensions for quasi-simultaneous welding in dependency to the scan repetition for using a conventional diode laser as well as a thulium fiber-laser (P_{Th}= 50 W, d_{Th} =2.1 mm) additionally (left column: weld depths (WDU, WDL) as well as the weld depth ratio (WDR), right column: weld widths (WWU, WWL) as well as the weld width ratio (WWR))

By comparing the experimental data with the simulations it is shown that the weld seam dimensions are computed in an adequate accuracy by using a thermo-mechanical coupled simulation. The thermal contact conductance is modelled as ideal in zones which are in contact and set to 0 as far as a gap greater than

10 microns occurs. Obviously it is also true, that the thermal contact conductance is depending on the surface roughness, the temperature as well as on the clamping pressure, which is neglected in this approach.

5. Conclusion and Outlook

A sufficient gap-bridging capability is of great interest in laser transmission welding, since an insufficiency can result in a reduced weld seam quality. In order to improve the gap-bridging capability, a secondary laser can be used additionally. In this investigation a conventional diode laser is used in combination with a thulium fiber-laser. For contour and quasi-simultaneous welding it is shown, that the weld seam is shifted towards the upper joining partner by using a thulium fiber-laser in addition. The experimental results are compared with thermo-mechanical coupled simulations, in which the thermal contact conductance between the joining partners is set in dependency of the contact situation. The simulation results fit with an adequate accuracy. As of now, effects on the thermal contact conductance like surface roughness, temperature and pressure dependencies are neglected. Based on the given results the process models can be used to derive adequate process parameter settings in order to investigate the effect of a secondary laser on gap-bridging, residual stresses and joint strength for several different thermoplastics in further experimental studies.

Acknowledgement

The authors want to thank the “Bayerisches Staatsministerium für Wirtschaft und Medien, Energie und Technologie” for funding the project „3D-LASPYRINT-Scanner“, and the German Research Foundation (DFG) for funding this work (Schm2115/31-1, Scho551/20-1).

References

Aden, M., Liviany, F., Olowinsky, A., 2013. Joint Strength for Laser Transmission Welding of Thermoplastics: A Simulation Approach, International Polymer Processing 28, p. 79-83.

Bates, P. J., Okoro, T. B., Chen, M., 2015. Thermal degradation of PC and PA6 during laser transmission welding, Welding in the World 59, p. 381-390.

Chen, M., Zak, G., Bates, P. J., Baylis, B., McLeod, M., 2011, Experimental Study on Gap Bridging in Contour Laser Transmission Welding of Polycarbonate and Polyamide, Polymer Engineering and Science 51, p. 1626-1635.

Devrient, M., Kern, M., Jaeschke, P., Stute, U., Haferkamp, H., Schmidt, M., 2013, Experimental Investigation of Laser Transmission Welding of Thermoplastics with Part-Adapted Temperature Fields, Physics Procedia 41, p. 59-69.

Geiger, M., Frick, T., Schmidt, M., 2009. Optical properties of plastics and their role for the modelling of the laser transmission welding process, Production Engineering Research and Development 3, p. 49-55.

Hofmann, A., Hierl, S., 2005. “Hybrid laser plastic welding”, Lasers in Manufacturing LIM. Munich, Germany, p. 215-218.

Hofmann, A., 2006. Hybrides Laserdurchstrahlschweißen von Kunststoffen, Meisenbach, Bamberg.

Majumdar, A., Lecroe B., D’Alvise L., 2015. “Thermal analysis of Laser Transmission Welding of thermoplastics: indicators of weld seam quality”, Lasers in Manufacturing LIM. Munich, Germany.

Sooriyapiragasam, S., Hopmann, C., 2016. Modelling of the heating process during the laser transmission welding of thermoplastics and calculation of the resulting stress distribution, Welding in the World 60, p. 777-791.

Liu, X., Liu, W., Meng, D., Wang, X., 2015. Simulation and experimental study of laser transmission welding considering the influence of interfacial contact status, Materials and Design 92, p. 246-260.

Piili, H., Taimisto, L., Purtonen, T., Laakso P., Salminen, A., 2009. “Computer simulation of quasi-simultaneous welding process of polycarbonate”, ICALEO 2009. Orlando, USA, paper #M407.

Potente, H., Wilke, L., Ridder, H., Mahnken, R., Shaban, A., 2008. Simulation of the Residual Stresses in the Contour Laser Welding of Thermoplastics, Polymer Engineering and Science 48, p. 767-773.

Schmailzl, A., Hierl, S., Sieben, M., Brunnecker, F., 2013. Using FE calculation for the optimisation of the clamping pressure distribution in the case of the laser transmission welding of complex components, JOINING PLASTICS 7 (1), p. 30-34.

Schkutow, A., Frick, T., 2016. Influence of Adapted Wavelengths on Temperature Fields and Melt Pool Geometry in Laser Transmission Welding, Physics Procedia 83, p. 1055-1063.

Wilke, L., Potente, H., Schnieders, J., 2008. Simulation of Quasi-Simultaneous and Simultaneous Laser Welding, Welding in the World 52, p. 56-66.

Zoubeir, T., Elhem G., 2010. Numerical study of laser diode transmission welding of a polypropylene mini-tank: Temperature field and residual stresses distribution, Polymer Testing 30, p. 23-33.